

# Theory and FE-analysis for structures with large deformation under magnetic loading

I. Münch<sup>1</sup>, W. Wagner

P. Neff

Institut für Baustatik  
Universität Karlsruhe (TH)  
Kaiserstraße 12  
76131 Karlsruhe  
Germany

FB Mathematik  
Technische Universität Darmstadt  
Schlossgartenstraße 7  
64289 Darmstadt  
Germany

**Abstract** We introduce and discuss a reduced micropolar continuum theory to simulate structures with large deformations under magnetic loading. Three numerical examples show the motivation of this model and its use in practical applications.

The question of how to choose the micropolar material parameters is addressed. We use that a finite strain micropolar model would reduce to classical elasticity in the absence of curvature effects and body couples and for certain parameter ranges. This gives us information about a proper choice of material parameters. Thus, we introduce in fact a nearly classical model, but with the feature to cover large deformations and non-classical types of loading.

As in shell theories, our continuum theory treats angular momentum as an explicit complementary principle. Thus, net couples - the typical loading of magnetized bodies in a magnetic field - can be modelled. Note that, in this case, the possibility for nonsymmetric Cauchy stresses is required for equilibrium, unlike classical shell theories.

Micropolar theories are not commonly used, by comparison to the Boltzmann continuum. One reason may be that micropolar theories often require greater modelling effort without significant advantage. However, the simplicity of introducing physical effects like magnetic loading compensates those efforts.

**Key words:** Magnetic loading, large deformation, extended continuum theory, finite element analysis, micropolar, Cosserat theory, magnetic switch, magnetic valve

## 1 Introduction

Rare earth metals like Neodymium have become important elements in powerful magnets, as they are affordable and allow for high remanent magnetization. The well known **Neodymium Iron Boron (NIB)** magnets  $\text{Ne}_2\text{Fe}_{14}\text{B}$  can be produced with a magnetic energy product up to  $54 \cdot 7.958 \text{ kJ/m}^3 = 54 \text{ MGOe}$  (Mega Gauss-Oersteds). This means a possible static remanent magnetic field of about 1.5 T (Tesla).

On the other hand, these magnets are very fragile, so they are often plated with a protective coating of metals such as nickel or encased in plastic or rubber to lessen the risk of breakage. Another idea is to bond small **NIB** particles (about 0.02 mm in diameter) within an elastomer matrix. Such flexible and strong magnetic materials can be used for switches or valves as our numerical examples will show in Section 5.

---

<sup>1</sup>Corresponding author. Tel.: +49 721 608 2280; fax: +49 721 608 6015, E-mail address: im@bs.uka.de

The central point of this paper is an appropriate continuum theory to predict the behaviour of flexible magnetic materials undergoing large deformation. For simplicity we assume elastic behaviour. The focus of this work lies in the magnetic loading and the resulting nonlinear behaviour during large deformation.

The outline of the paper is as follows. In Section 2 the basic equations to handle exact rotations within this work are summarized. Then, the governing equations for the theory are presented and material parameters are discussed. Section 3 develops a finite element formulation that can be used to numerically solve boundary value problems. The model is extended in Section 4 with deformation dependent net couples, which represent magnetic loading among others. Finally, numerical examples in Section 5 and a summary in Section 6 complete the work.

## 2 A micropolar continuum theory

A general micropolar model introduce an additional rotation field similar to the rotational degrees of freedom in shells, see e.g. Wisniewski [26]. It appears in the kinematical equations of our formulation as an exact rotation  $\bar{\mathbf{R}} \in \text{SO}(3)$ . This is a source for nonlinearity in the model which allows easily for large deformation.

It is useful to connect  $\bar{\mathbf{R}}$  to its eigenvector<sup>2</sup>  $\bar{\boldsymbol{\alpha}}$ , which is therefore no element of the ABEL group. Thus,  $\bar{\boldsymbol{\alpha}}_1 + \bar{\boldsymbol{\alpha}}_2$  is meaningless and  $\bar{\boldsymbol{\alpha}}$  is in the true sense of the word a pseudo vector. However, we name  $\bar{\boldsymbol{\alpha}}$  rotational vector field, it is also known as EULER-RODRIGUES rotation vector. Any rotation  $\bar{\mathbf{R}} \in \text{SO}(3)$  can be represented as an exponential function and further as an absolut converging matrix potential progression according to

$$\bar{\mathbf{R}} = \exp[\bar{\mathbf{A}}] = \mathbb{1} + \frac{\bar{\mathbf{A}}}{1!} + \frac{\bar{\mathbf{A}}^2}{2!} + \frac{\bar{\mathbf{A}}^3}{3!} + \frac{\bar{\mathbf{A}}^4}{4!} + \dots \quad (1)$$

The skewsymmetric tensor  $\bar{\mathbf{A}} \in \mathfrak{so}(3)$  (the infinitesimal microrotation matrix) provide an isomorphism to the rotational vector field via

$$\bar{\mathbf{A}} = \begin{pmatrix} 0 & -\alpha_3 & \alpha_2 \\ \alpha_3 & 0 & -\alpha_1 \\ -\alpha_2 & \alpha_1 & 0 \end{pmatrix}, \quad \bar{\boldsymbol{\alpha}} := \text{axl}[\bar{\mathbf{A}}] = \begin{pmatrix} \alpha_1 \\ \alpha_2 \\ \alpha_3 \end{pmatrix}. \quad (2)$$

Thus, for any  $\mathbf{u} \in \mathbb{R}^3$  we have  $\bar{\mathbf{A}} \mathbf{u} = \bar{\boldsymbol{\alpha}} \times \mathbf{u}$  with the usual vector cross product reading in index notation  $\bar{\boldsymbol{\alpha}} \times \mathbf{u} = \epsilon_{ijk} \bar{\alpha}_i u_j \mathbf{e}_k$ . Beside the power series of  $\bar{\mathbf{R}}$  in Eq. (1) there is also the possibility of a condensed relation  $\mathfrak{so}(3) \mapsto \text{SO}(3)$  given by

$$\bar{\mathbf{R}} = \mathbb{1} + \frac{\sin\|\bar{\boldsymbol{\alpha}}\|}{\|\bar{\boldsymbol{\alpha}}\|} \bar{\mathbf{A}} + \frac{1 - \cos\|\bar{\boldsymbol{\alpha}}\|}{\|\bar{\boldsymbol{\alpha}}\|^2} \bar{\mathbf{A}}^2. \quad (3)$$

The differentiation of rotations on  $\text{SO}(3)$  shows a peculiarity, which is essential for their treatment in a variational, respectively numerical formulation. One result of the Lie-group theory is the differential  $D$  of the matrix exponential function in analytical form, see Hofmann

---

<sup>2</sup> $\bar{\mathbf{R}} \bar{\boldsymbol{\alpha}} = 1 \bar{\boldsymbol{\alpha}}$

& Morris [13] Lemma 5.2. The Taylor series of a rotation field  $\bar{\mathbf{R}}$  at  $\bar{\mathbf{A}} \in \mathfrak{so}(3)$  for an increment  $\mathbf{H} \in \mathfrak{so}(3)$  reads

$$\begin{aligned}\bar{\mathbf{R}}(\bar{\mathbf{A}} + \mathbf{H}) &= \exp[\bar{\mathbf{A}} + \mathbf{H}] = \exp[\bar{\mathbf{A}}] + D \exp[\bar{\mathbf{A}}] \cdot \mathbf{H} + o(\mathbf{H}) \\ &= \bar{\mathbf{R}}(\bar{\mathbf{A}}) + \exp[\bar{\mathbf{A}}] \cdot \left[ \sum_{i=1}^{\infty} \frac{1}{i!} (-\text{adj}[\bar{\mathbf{A}}])^{i-1} \right] \cdot \mathbf{H} + o(\mathbf{H}),\end{aligned}\quad (4)$$

with the operator  $\text{adj}[\mathbf{A}] \in \text{Lin}[\mathfrak{so}(3), \mathfrak{so}(3)]$ ,  $\text{adj}[\mathbf{A}] \cdot \mathbf{H} := \mathbf{A} \cdot \mathbf{H} - \mathbf{H} \cdot \mathbf{A}$ .

If the increment  $\mathbf{H}$  of the argument is small, for example in a variation, one can neglect terms of higher order  $o(\mathbf{H})$  and the variation of a rotational field  $\delta\bar{\mathbf{R}}$  can be identified as

$$\exp[\bar{\mathbf{A}}] \cdot \underbrace{\left[ \sum_{i=1}^{\infty} \frac{1}{i!} (-\text{adj}[\bar{\mathbf{A}}])^{i-1} \right] \cdot \mathbf{H}}_{:= \mathbf{B} \in \mathfrak{so}(3)} = \bar{\mathbf{R}}(\bar{\mathbf{A}}) \cdot \mathbf{B} =: \delta\bar{\mathbf{R}}.\quad (5)$$

Note that the test function  $\mathbf{B} \in \mathfrak{so}(3)$  is not equivalent to the increment  $\mathbf{H} \in \mathfrak{so}(3)$ . However, this is meaningless regarding the arbitrariness of test functions. Further, it is possible to conjugate the expression in Eq. (5), such that

$$\delta\bar{\mathbf{R}}(\bar{\mathbf{A}}) = \bar{\mathbf{R}}(\bar{\mathbf{A}}) \cdot \mathbf{B} = (\bar{\mathbf{R}} \cdot \mathbf{B}) \cdot \underbrace{(\bar{\mathbf{R}}^T \cdot \bar{\mathbf{R}})}_{\mathbb{1}} = \underbrace{(\bar{\mathbf{R}} \cdot \mathbf{B} \cdot \bar{\mathbf{R}}^T)}_{:= \mathbf{W} \in \mathfrak{so}(3)} \cdot \bar{\mathbf{R}} = \mathbf{W} \cdot \bar{\mathbf{R}}.\quad (6)$$

Within the subsequent numerical formulation Eq. (6) can help to gain more compact expressions. Taking usual mathematical principles for variation and differentiation into account leads to the observation that the linearization of  $\bar{\mathbf{R}}$  reads  $\Delta\bar{\mathbf{R}}(\bar{\mathbf{A}}) = \mathbf{Y} \cdot \bar{\mathbf{R}}$ ,  $\mathbf{Y} \in \mathfrak{so}(3)$ . For more details and for numerical treatment of  $\bar{\mathbf{R}}$  we refer to [2, 16, 22, 23].

The rotational field  $\bar{\mathbf{R}}$  is geometrically coupled to the gradient of the deformation  $\varphi$  through the first Cosserat [5] strain measure, which is defined by

$$\bar{\mathbf{U}} := \bar{\mathbf{R}}^T \text{Grad}[\varphi] = \bar{\mathbf{R}}^T \mathbf{F}, \quad \bar{\mathbf{U}} \in \text{GL}^+(3) \quad \Leftrightarrow \quad \mathbf{F} = \bar{\mathbf{R}} \bar{\mathbf{U}}.\quad (7)$$

In this paper we do not follow the common practice in micropolar theories (e.g. [6, 9, 12, 14, 18]) to define a curvature measure  $\mathfrak{C}$  and a curvature energy density  $W_{\text{curv}}(\mathfrak{C}, L_c)$ . This would involve gradients of  $\bar{\mathbf{R}}$  and take deformation effects of higher order into account. Such higher order effects can of course appear and usually lead to couple stresses and to size effects, see e.g. Fleck et al. [10]. The micropolar theory straight offers itself as a tool to be associated with size effects. Nevertheless, we exclude this here deliberately to exclude any unclearness in our choice of material parameters. In other words, we consider an internal length scale  $L_c = 0$  and therefore  $W_{\text{curv}} = 0$ .

In principle, the strain  $\bar{\mathbf{U}}$  in Eq. (7) is possibly nonsymmetric and we emphasize this difference to classical symmetric strain measures. Thus, the inner strain energy density

$$W_{\text{mp}}(\bar{\mathbf{U}}) = \mu \|\text{sym}[\bar{\mathbf{U}} - \mathbb{1}]\|^2 + \mu_c \|\text{skew}[\bar{\mathbf{U}}]\|^2 + \frac{\lambda}{4} \left( (\det[\bar{\mathbf{U}}] - 1)^2 + \left( \frac{1}{\det[\bar{\mathbf{U}}]} - 1 \right)^2 \right)\quad (8)$$

contains the marked split into symmetrical and skew-symmetrical strain components, see e.g. Neff [17]. Symmetric parts of  $\bar{\mathbf{U}}$  are penalized with the classical Lamé parameter  $\mu$  and volumetric parts with  $\lambda$ , which is consistent to classical elasticity theories. Because of  $\det[\bar{\mathbf{U}}] = \det[\bar{\mathbf{R}}^T \mathbf{F}] = \det[\mathbf{F}]$  rotations are in reality absent in the volumetric part of the inner strain energy as it is physically reasonable.<sup>3</sup>

Skewsymmetric parts of  $\bar{\mathbf{U}}$  are penalized with the Cosserat couple modulus  $\mu_c$ . This term is responsible for the interaction between equilibrium of momentum and angular momentum. The interaction is not sensitive, roughly spoken, it is present or not. We are dealing here with a problem of geometrical cloupling - do not think about mixed field problems where the coupling happens sensitive through phenomenological constitutive equations. Instead of the second term in Eq. (8) we could also use a side condition  $\bar{\mathbf{R}} = \mathbf{R}$ , with<sup>4</sup>  $\mathbf{R} = \text{polar}[\mathbf{F}]$ . But this would lead algorithmically to a comparable formulation.

Thus,  $\mu_c$  is here not a material parameter but a modelling parameter, appearing for the convenience of the numerical implementation and the possibility to treat body couples. In the absence of curvature energy (internal length scale  $L_c = 0$ ) the couple modulus guarantees for classical elasticity if  $\mu_c \geq \mu$  and if there are no boundary conditions **and no body couples** on  $\bar{\mathbf{R}}$ , see Neff et al. [21], Bufler [3], Simo et al. [11]. Since it is our aim to apply magnetic loading via body couples, our model is not a classical model.

This is useful, if one strives for a classical elasticity formulation and couples algorithmically rotational degrees of freedom to the macroscopic deformation in a strong way.

We consider for all our numerical examples in this paper  $\mu_c = \mu$ . Note that we obtain the same results for  $\mu_c > \mu$ , which has been also numerically proven for  $\mu_c \in [\mu, 1000\mu]$ . Of course,  $\mu_c = \mu$  leads to better conditions within the finite element stiffness matrix than  $\mu_c = 1000\mu$  would do. We stress again that the appearance of the rotational field is a numerical device only which nevertheless allows to take into account non-classical loading in a straight-forward manner.

### 3 Variational formulation and FE-approximation

Formally, a two field problem results from the assumed kinematic, which is posed in a variational setting. The task is to find a pair  $(\varphi, \bar{\mathbf{R}})$  minimizing the energy

$$\Pi(\varphi, \bar{\mathbf{R}}) = \int_{\mathcal{B}_0} W_{\text{mp}}(\mathbf{F}, \bar{\mathbf{R}}) \, dV + \Pi^{\text{ext}}(\varphi, \bar{\mathbf{R}}) \rightarrow \min. \text{ w.r.t. } (\varphi, \bar{\mathbf{R}}), \quad (9)$$

together with the Dirichlet boundary condition of place for the deformation  $\varphi|_{\Gamma} = g_D$  on  $\Gamma \subset \partial\mathcal{B}_0$  and the induced (free) Neumann-type boundary condition for the rotation  $\bar{\mathbf{R}}$ .

The variational form of Eq. (9) defines

$$G := \delta\Pi(\varphi, \delta\varphi, \bar{\mathbf{R}}, \delta\bar{\mathbf{R}}) = \int_{\mathcal{B}_0} \left\langle \frac{\partial W_{\text{mp}}}{\partial \bar{\mathbf{U}}}, \delta\bar{\mathbf{U}} \right\rangle \, dV + \delta\Pi^{\text{ext}}(\varphi, \delta\varphi, \bar{\mathbf{R}}, \delta\bar{\mathbf{R}}) \stackrel{!}{=} 0, \quad (10)$$

<sup>3</sup>This is a sufficient motivation to use  $\det[\bar{\mathbf{U}}]$  in Eq. 8. However, in other applications of this model further reasons for  $\det[\bar{\mathbf{U}}]$  appear.

<sup>4</sup> $\text{polar}[\mathbf{F}]$  is the orthogonal part of the polar decomposition of  $\mathbf{F}$

for all admissible variations  $\delta\boldsymbol{\varphi}$  and  $\delta\bar{\mathbf{R}}$ . The operator  $\langle a, b \rangle$  denotes the scalar product between admissible arguments  $a$  and  $b$ . Mechanical stresses appear in Eq. (10) according to

$$\mathbf{T} := \frac{\partial W_{\text{mp}}}{\partial \bar{\mathbf{U}}} = 2 \underbrace{\mu \text{sym}[\bar{\mathbf{U}} - \mathbb{1}] + 2 \mu_c \text{skew}[\bar{\mathbf{U}} - \mathbb{1}]}_{:=\mathbf{T}^{\text{lin}}} + \underbrace{C_{\text{det}}(\bar{\mathbf{U}}) \bar{\mathbf{U}}^{-T}}_{:=\mathbf{T}^{\text{nonli}}}, \quad (11)$$

with the nonlinear factor

$$C_{\text{det}}(\bar{\mathbf{U}}) := \frac{\lambda}{2} \left( (\det[\bar{\mathbf{U}}])^2 - \det[\bar{\mathbf{U}}] + \frac{1}{\det[\bar{\mathbf{U}}]} - \frac{1}{(\det[\bar{\mathbf{U}}])^2} \right). \quad (12)$$

A compact notation  $\mathbf{T}^{\text{lin}} = \mathbf{C} : (\bar{\mathbf{U}} - \mathbb{1}) = (\bar{\mathbf{U}} - \mathbb{1}) : \mathbf{C}$  is also given for the linear part of stresses by using the compliance matrix

$$\mathbf{C} := \mu (\delta_{ik} \delta_{jl} + \delta_{il} \delta_{jk}) + \mu_c (\delta_{ik} \delta_{jl} - \delta_{il} \delta_{jk}) \mathbf{e}_i \otimes \mathbf{e}_j \otimes \mathbf{e}_k \otimes \mathbf{e}_l. \quad (13)$$

Introducing a displacement vector field  $\mathbf{u}$  with  $\text{Grad}[\mathbf{u}] = \mathbf{F}$ , we define  $\text{Grad}[\delta\mathbf{u}] := \delta\mathbf{F} = \delta\boldsymbol{\varphi}$  and by consideration of Eq. (6) and Eq. (7) get

$$\delta\bar{\mathbf{U}} = \delta(\bar{\mathbf{R}}^T \mathbf{F}) = \bar{\mathbf{R}}^T \mathbf{W}^T \mathbf{F} + \bar{\mathbf{R}}^T \delta\mathbf{F}. \quad (14)$$

The external energy  $\Pi^{\text{ext}}$  may contain contributions from net forces  $\mathbf{b}_0$ , net couples  $\mathbf{l}_0$ , surface tractions  $\mathbf{t}_0$  and surface couples  $\mathbf{c}_0$ . For the moment we assume these contributions to be independent of  $\boldsymbol{\varphi}$  and  $\bar{\mathbf{R}}$ . Then Eq. (10) ends up in the averaged balance of momentum

$$\int_{\mathcal{B}_0} \langle \bar{\mathbf{T}}, \bar{\mathbf{R}}^T \delta\mathbf{F} \rangle - \langle \mathbf{b}_0, \delta\mathbf{u} \rangle dV - \int_{\partial\mathcal{B}_0} \langle \mathbf{t}_0, \delta\mathbf{u} \rangle dA = 0, \quad (15)$$

as well as the averaged balance of angular momentum

$$\int_{\mathcal{B}_0} \langle \bar{\mathbf{T}}, \bar{\mathbf{R}}^T \mathbf{W}^T \mathbf{F} \rangle - \langle \mathbf{l}_0, \mathbf{w} \rangle dV - \int_{\partial\mathcal{B}_0} \langle \mathbf{c}_0, \mathbf{w} \rangle dA = 0. \quad (16)$$

The isomorphism from Eq. (2) is also used in Eq. (16) to define  $\mathbf{w} := \text{axl}[\mathbf{W}]$ .

Within the finite element method, the structure, its displacement field  $\mathbf{u}$  and its rotational vector field  $\bar{\boldsymbol{\alpha}}$  is approximated by a finite number (*nel*) of initial nodal position vectors  $\mathbf{X}^I$ , nodal displacements  $\mathbf{u}^I$  and nodal rotation vectors  $\bar{\boldsymbol{\alpha}}^I$ , combined with shape functions  $N^I$  via

$$\mathbf{X} = N^I \mathbf{X}^I, \quad \mathbf{u} = N^I \mathbf{u}^I, \quad \bar{\boldsymbol{\alpha}} = N^I \bar{\boldsymbol{\alpha}}^I. \quad (17)$$

In this paper standard index notation is used with summation implied over repeated indices. This holds also for superscripts  $I$  and  $J$ . We use the same procedure and shape functions for variations respectively increments of the displacement and rotation vector field according to

$$\delta\mathbf{u} = N^I \delta\mathbf{u}^I, \quad \delta\bar{\boldsymbol{\alpha}} = N^I \delta\bar{\boldsymbol{\alpha}}^I, \quad \Delta\mathbf{u} = N^I \Delta\mathbf{u}^I, \quad \Delta\bar{\boldsymbol{\alpha}} = N^I \Delta\bar{\boldsymbol{\alpha}}^I. \quad (18)$$

Doing so, the body  $\mathcal{B}$  is divided into a finite number  $n_{\text{elm}}$  of substructures  $\mathcal{B}^e$  given by

$$\mathcal{B} = \bigcup_{e=1}^{n_{\text{elm}}} \mathcal{B}^e. \quad (19)$$

The properties and fields of the body are divided on these substructures as well, thus the same assembling operator  $\bigcup$  appears also there.

Process vectors for the primary variables  $\mathbf{p} = (\mathbf{u}, \bar{\boldsymbol{\alpha}})$ ,  $\delta\mathbf{p} = (\delta\mathbf{u}, \mathbf{w})$  and  $\Delta\mathbf{p} = (\Delta\mathbf{u}, \mathbf{y})$  are used to reformulate Eq. (10) after linearization at the evolution point  $\mathbf{p}^*$  of a Taylor series

$$\begin{aligned} \text{Lin } G^h(\mathbf{p}^*, \delta\mathbf{p}, \Delta\mathbf{p}) &= G^h(\mathbf{p}^*, \delta\mathbf{p}) + DG^h(\mathbf{p}^*, \delta\mathbf{p}) \cdot \Delta\mathbf{p} \stackrel{!}{=} 0 \\ &\Leftrightarrow DG^h(\mathbf{p}^*, \delta\mathbf{p}) \cdot \Delta\mathbf{p} = -G^h(\mathbf{p}^*, \delta\mathbf{p}). \end{aligned} \quad (20)$$

Assembling only nodal values within the process vectors and separating  $\delta\mathbf{p}$  and  $\Delta\mathbf{p}$ , Eq. (20) results in the usual finite element equation system

$$\delta\mathbf{p} \cdot \mathbf{K}_T(\mathbf{p}^*) \cdot \Delta\mathbf{p} = \delta\mathbf{p} \cdot \mathbf{R}_V(\mathbf{p}^*) \quad \rightarrow \quad \mathbf{K}_T(\mathbf{p}^*) \cdot \Delta\mathbf{p} = \mathbf{R}_V(\mathbf{p}^*), \quad (21)$$

which gives an outline for the following detailed description. We start with the right hand side of Eq. (21), given by

$$-G^h(\mathbf{p}^*, \delta\mathbf{p}) = \int_{\mathcal{B}_0} \langle \mathbf{b}_0, \delta\mathbf{u} \rangle + \langle \mathbf{l}_0, \mathbf{w} \rangle dV + \int_{\partial\mathcal{B}_0} \langle \mathbf{t}_0, \delta\mathbf{u} \rangle + \langle \mathbf{c}_0, \mathbf{w} \rangle dA - \int_{\mathcal{B}_0} \langle \mathbf{T}^*, \delta\bar{\mathbf{U}}^* \rangle dV. \quad (22)$$

The first PIOLA-KIRCHHOFF stress  $\mathbf{S}_1 = \bar{\mathbf{R}} \mathbf{T}$  appears within the virtual work expression

$$\langle \mathbf{T}, \delta\bar{\mathbf{U}} \rangle = \langle \mathbf{T}, \bar{\mathbf{R}}^T \delta\mathbf{F} + \bar{\mathbf{R}}^T \mathbf{W}^T \mathbf{F} \rangle = \langle \bar{\mathbf{R}} \mathbf{T}, \delta\mathbf{F} + \mathbf{W}^T \mathbf{F} \rangle = \langle \mathbf{S}_1, \delta\mathbf{F} \rangle + \langle \mathbf{S}_1, \mathbf{W}^T \mathbf{F} \rangle. \quad (23)$$

Fields in Eq. (23) and further expressions always concern to  $\mathbf{p}^*$ , thus, if it is not necessary, we omit the accompanying  $\star$ . Separation of  $\delta\mathbf{u}$  respectively of  $\mathbf{w}$  in Eq. (23) follows via

$$\langle \mathbf{S}_1, \delta\mathbf{F} \rangle = \langle \delta\mathbf{F}, \mathbf{S}_1 \rangle = \delta\mathbf{u}^I \otimes \text{Grad}[N^I] : \mathbf{S}_1 = \delta\mathbf{u}^I \cdot \underbrace{\mathbf{S}_1 \cdot \text{Grad}[N^I]}_{:=\mathbf{B}_\alpha^I}, \quad (24)$$

$$\langle \mathbf{S}_1, \mathbf{W}^T \mathbf{F} \rangle = \langle -\mathbf{W}, \mathbf{S}_1 \mathbf{F}^T \rangle = (\mathbf{w} \cdot \boldsymbol{\epsilon}) : (\mathbf{S}_1 \cdot \mathbf{F}^T) = \mathbf{w}^I \cdot \underbrace{\boldsymbol{\epsilon} : \mathbf{S}_1 \cdot \mathbf{F}^T N^I}_{:=\mathbf{B}_\beta^I}. \quad (25)$$

Together with the external virtual loadings in Eq. (22) it results in the right hand side

$$-G^h(\mathbf{p}^*, \delta\mathbf{p}^*) = \bigcup_{e=1}^{n_{\text{elm}}} \delta\mathbf{u}^I \cdot \mathbf{R}_V^{eI} + \mathbf{w}^I \cdot \mathbf{R}_V^e \quad (26)$$

of the finite element formulation with the element vectors

$$\mathbf{R}_V^{eI} = \int_{\mathcal{B}_0^e} \mathbf{b}_0 N^I - \mathbf{B}_\alpha^I dV + \int_{\partial\mathcal{B}_0^e} \mathbf{t}_0 N^I dA, \quad \mathbf{R}_V^e = \int_{\mathcal{B}_0^e} \mathbf{l}_0 N^I - \mathbf{B}_\beta^I dV + \int_{\partial\mathcal{B}_0^e} \mathbf{c}_0 N^I dA. \quad (27)$$

The left hand side of Eq. (20) describes linear changes of the variational formulation at  $\mathbf{p}^*$  by

$$DG^h(\mathbf{p}^*, \delta\mathbf{p}^*) \cdot \Delta\mathbf{p} = \int_{\mathcal{B}_0} \Delta \langle \mathbf{T}^*, \delta\bar{\mathbf{U}}^* \rangle dV = \int_{\mathcal{B}_0} (\langle \Delta\mathbf{T}^*, \delta\bar{\mathbf{U}}^* \rangle + \langle \mathbf{T}^*, \Delta\delta\bar{\mathbf{U}}^* \rangle) dV. \quad (28)$$

The operator  $\Delta$  denotes an incremental difference to the point of evolution  $\mathbf{p}^*$ . In Section 4 we concentrate on deformation dependent magnetic loading, but for the moment we consider

external work to be deformation independent. Therefore, only terms of inner virtual work appear in Eq. (28). For a detailed calculation of  $\langle \Delta \mathbf{T}^*, \delta \bar{\mathbf{U}}^* \rangle$  we use the decomposition of stresses in linear and nonlinear parts and obtain for the linear part

$$\begin{aligned} \langle \Delta \mathbf{T}^{\text{lin}}, \delta \bar{\mathbf{U}} \rangle &= (\bar{\mathbf{R}}^T \delta \mathbf{F}) : \mathbb{C} : (\bar{\mathbf{R}}^T \Delta \mathbf{F}) + (\bar{\mathbf{R}}^T \delta \mathbf{F}) : \mathbb{C} : (\bar{\mathbf{R}}^T \mathbf{Y}^T \mathbf{F}) \\ &\quad + (\bar{\mathbf{R}}^T \mathbf{W}^T \mathbf{F}) : \mathbb{C} : (\bar{\mathbf{R}}^T \Delta \mathbf{F}) + (\bar{\mathbf{R}}^T \mathbf{W}^T \mathbf{F}) : \mathbb{C} : (\bar{\mathbf{R}}^T \mathbf{Y}^T \mathbf{F}). \end{aligned} \quad (29)$$

Since the nonlinear stress  $\mathbf{T}^{\text{nili}}$  is orthogonal to  $\bar{\mathbf{R}}^T \mathbf{W}^T \mathbf{F}$ , according to

$$\begin{aligned} \langle \mathbf{T}^{\text{nili}}, \bar{\mathbf{R}}^T \mathbf{W}^T \mathbf{F} \rangle &= C_{\text{det}} \langle \bar{\mathbf{R}} \bar{\mathbf{U}}^{-T}, \mathbf{W}^T \mathbf{F} \rangle = C_{\text{det}} \langle \bar{\mathbf{R}} \bar{\mathbf{R}}^T \mathbf{F}^{-T}, \mathbf{W}^T \mathbf{F} \rangle \\ &= C_{\text{det}} \langle \mathbf{F}^{-T} \mathbf{F}^T, \mathbf{W}^T \rangle = C_{\text{det}} \langle \mathbb{1}, \mathbf{W}^T \rangle = 0, \end{aligned} \quad (30)$$

it holds

$$\langle \Delta \mathbf{T}^{\text{nili}}, \delta \bar{\mathbf{U}} \rangle = \langle \Delta \mathbf{T}^{\text{nili}}, \bar{\mathbf{R}}^T \delta \mathbf{F} + \bar{\mathbf{R}}^T \mathbf{W}^T \mathbf{F} \rangle = \langle \Delta \mathbf{T}^{\text{nili}}, \bar{\mathbf{R}}^T \delta \mathbf{F} \rangle \quad (31)$$

and further

$$\langle \bar{\mathbf{T}}^{\text{nili}}, \Delta \delta \bar{\mathbf{U}} \rangle = \langle \bar{\mathbf{T}}^{\text{nili}}, \Delta(\bar{\mathbf{R}}^T \mathbf{W}^T \mathbf{F} + \bar{\mathbf{R}}^T \delta \mathbf{F}) \rangle = \langle \bar{\mathbf{T}}^{\text{nili}}, \Delta \bar{\mathbf{R}}^T \delta \mathbf{F} \rangle = \langle \bar{\mathbf{T}}^{\text{nili}}, \bar{\mathbf{R}}^T \mathbf{Y}^T \delta \mathbf{F} \rangle. \quad (32)$$

In Eq. (32) we made use of Eq. (6), which is also valid for

$$\Delta \delta \bar{\mathbf{U}} = \Delta(\bar{\mathbf{R}}^T \mathbf{W}^T \mathbf{F} + \bar{\mathbf{R}}^T \delta \mathbf{F}) = \bar{\mathbf{R}}^T \mathbf{Y}^T \mathbf{W}^T \mathbf{F} + \bar{\mathbf{R}}^T \mathbf{W}^T \Delta \mathbf{F} + \bar{\mathbf{R}}^T \mathbf{Y}^T \delta \mathbf{F}. \quad (33)$$

This brings us to details of the second term in Eq. (28), given by

$$\begin{aligned} \langle \mathbf{T}, \Delta \delta \bar{\mathbf{U}} \rangle &= \langle \mathbf{T}^{\text{lin}}, \bar{\mathbf{R}}^T \mathbf{Y}^T \mathbf{W}^T \mathbf{F} \rangle + \langle \mathbf{T}^{\text{lin}}, \bar{\mathbf{R}}^T \mathbf{W}^T \Delta \mathbf{F} \rangle + \langle \mathbf{T}^{\text{lin}}, \bar{\mathbf{R}}^T \mathbf{Y}^T \delta \mathbf{F} \rangle + \langle \mathbf{T}^{\text{nili}}, \bar{\mathbf{R}}^T \mathbf{Y}^T \delta \mathbf{F} \rangle \\ &= \langle \bar{\mathbf{R}} \mathbf{T}^{\text{lin}}, \mathbf{Y}^T \mathbf{W}^T \mathbf{F} \rangle + \langle \bar{\mathbf{R}} \mathbf{T}^{\text{lin}}, \mathbf{W}^T \Delta \mathbf{F} \rangle + \langle \bar{\mathbf{R}} \mathbf{T}, \mathbf{Y}^T \delta \mathbf{F} \rangle \\ &= \langle \mathbf{S}_1^{\text{lin}}, \mathbf{Y} \mathbf{W} \mathbf{F} \rangle + \langle \mathbf{S}_1^{\text{lin}}, \mathbf{W}^T \Delta \mathbf{F} \rangle + \langle \mathbf{S}_1, \mathbf{Y}^T \delta \mathbf{F} \rangle. \end{aligned} \quad (34)$$

The increment of the nonlinear stress reads

$$\Delta \bar{\mathbf{T}}^{\text{nili}} = \Delta(C_{\text{det}} \bar{\mathbf{U}}^{-T}) = \hat{C}_{\text{det}} \langle \bar{\mathbf{U}}^{-T}, \Delta \bar{\mathbf{U}} \rangle \bar{\mathbf{U}}^{-T} - C_{\text{det}} \bar{\mathbf{U}}^{-T} \Delta \bar{\mathbf{U}}^T \bar{\mathbf{U}}^{-T} \quad (35)$$

with  $C_{\text{det}}$  from Eq. (12) and

$$\hat{C}_{\text{det}} := \frac{\lambda}{2} \left( 2(\det[\bar{\mathbf{U}}])^2 - \det[\bar{\mathbf{U}}] - \frac{1}{\det[\bar{\mathbf{U}}]} + \frac{2}{(\det[\bar{\mathbf{U}}])^2} \right). \quad (36)$$

Inserting Eq. (35) into Eq. (31) gives

$$\langle \Delta \mathbf{T}^{\text{nili}}, \bar{\mathbf{R}}^T \delta \mathbf{F} \rangle = \hat{C}_{\text{det}} \langle \delta \mathbf{F}, \mathbf{F}^{-T} \rangle \langle \bar{\mathbf{U}}^{-T}, \Delta \bar{\mathbf{U}} \rangle - C_{\text{det}} \langle \delta \mathbf{F}, \mathbf{F}^{-T} \Delta \bar{\mathbf{U}}^T \bar{\mathbf{U}}^{-T} \rangle. \quad (37)$$

Using

$$\begin{aligned} \langle \bar{\mathbf{U}}^{-T}, \Delta \bar{\mathbf{U}} \rangle &= \langle \bar{\mathbf{R}}^T \mathbf{F}^{-T}, \bar{\mathbf{R}}^T \mathbf{Y}^T \mathbf{F} \rangle + \langle \bar{\mathbf{R}}^T \mathbf{F}^{-T}, \bar{\mathbf{R}}^T \Delta \mathbf{F} \rangle \\ &= \langle \bar{\mathbf{R}} \bar{\mathbf{R}}^T \mathbf{F}^{-T} \mathbf{F}^T, \mathbf{Y}^T \rangle + \langle \bar{\mathbf{R}} \bar{\mathbf{R}}^T \mathbf{F}^{-T}, \Delta \mathbf{F} \rangle = \langle \mathbf{F}^{-T}, \Delta \mathbf{F} \rangle \end{aligned} \quad (38)$$

as well as

$$\begin{aligned}\mathbf{F}^{-T} \Delta \bar{\mathbf{U}}^T \bar{\mathbf{U}}^{-T} &= \mathbf{F}^{-T} (\bar{\mathbf{R}}^T \mathbf{Y}^T \mathbf{F} + \bar{\mathbf{R}}^T \Delta \mathbf{F})^T \bar{\mathbf{U}}^{-T} = \mathbf{F}^{-T} (\mathbf{F}^T \mathbf{Y} \bar{\mathbf{R}} + \Delta \mathbf{F}^T \bar{\mathbf{R}}) \bar{\mathbf{U}}^{-T} \\ &= \mathbf{Y} \bar{\mathbf{R}} \bar{\mathbf{U}}^{-T} + \mathbf{F}^{-T} \Delta \mathbf{F}^T \bar{\mathbf{R}} \bar{\mathbf{U}}^{-T} = \mathbf{Y} \mathbf{F}^{-T} + \mathbf{F}^{-T} \Delta \mathbf{F}^T \mathbf{F}^{-T}\end{aligned}\quad (39)$$

results in

$$\langle \Delta \mathbf{T}^{\text{nili}}, \bar{\mathbf{R}}^T \delta \mathbf{F} \rangle = \hat{C}_{\text{det}} \langle \delta \mathbf{F}, \mathbf{F}^{-T} \rangle \langle \mathbf{F}^{-T}, \Delta \mathbf{F} \rangle - C_{\text{det}} \langle \delta \mathbf{F}, \mathbf{Y} \mathbf{F}^{-T} \rangle - C_{\text{det}} \langle \delta \mathbf{F}, \mathbf{F}^{-T} \Delta \mathbf{F}^T \mathbf{F}^{-T} \rangle. \quad (40)$$

After allocating Eq. (28) we add up 10 terms from Eqs. (29), (34) and (40) for the stiffness matrix of the finite element formulation. Separation of  $\delta \mathbf{u}$ ,  $\mathbf{w}$ ,  $\Delta \mathbf{u}$  and  $\mathbf{y}$  similar as in Eqs. (24) and (25) results in

$$DG^h(\mathbf{p}^*, \delta \mathbf{p}^*) \cdot \Delta \mathbf{p} = \bigcup_{e=1}^{n_{\text{elm}}} \delta \mathbf{u}^I \cdot \left( \mathbf{K}_{\text{T}}^{eIJ} \cdot \Delta \mathbf{u}^J + \mathbf{K}_{\text{T}}^{eIJ} \cdot \mathbf{y}^J \right) + \mathbf{w}^I \cdot \left( \mathbf{K}_{\text{T}}^{eIJ} \cdot \Delta \mathbf{u}^J + \mathbf{K}_{\text{T}}^{eIJ} \cdot \mathbf{y}^J \right). \quad (41)$$

Together with the right hand side in Eq. (26) and considering arbitrary variational functions  $\delta \mathbf{u}$  and  $\mathbf{w}$ , the linear equation system from Eq. (21) holds if

$$\bigcup_{e=1}^{n_{\text{elm}}} \begin{bmatrix} uu & uy \\ \mathbf{K}_{\text{T}}^{eIJ} & \mathbf{K}_{\text{T}}^{eIJ} \\ wu & wy \\ \mathbf{K}_{\text{T}}^{eIJ} & \mathbf{K}_{\text{T}}^{eIJ} \end{bmatrix} \cdot \begin{pmatrix} \Delta \mathbf{u}^J \\ \mathbf{y}^J \end{pmatrix} = \bigcup_{e=1}^{n_{\text{elm}}} \begin{pmatrix} u \\ \mathbf{R}_V^{eI} \\ w \\ \mathbf{R}_V^{eI} \end{pmatrix}. \quad (42)$$

The element stiffness matrices

$$\begin{aligned}\mathbf{K}_{\text{T}}^{eIJ} &:= \int_{\mathcal{B}_0^e} \mathbf{B}_{\delta}^{IJ} + \mathbf{B}_{\theta}^{IJ} + \mathbf{B}_{\vartheta}^{IJ} \, dV, & \mathbf{K}_{\text{T}}^{eIJ} &:= \int_{\mathcal{B}_0^e} \mathbf{B}_{\epsilon}^{IJ} + \mathbf{B}_{\iota}^{IJ} + \mathbf{B}_{\varpi}^{IJ} \, dV \\ \mathbf{K}_{\text{T}}^{eIJ} &:= \int_{\mathcal{B}_0^e} (\mathbf{B}_{\epsilon}^{JI})^T + \mathbf{B}_{\lambda}^{IJ} \, dV, & \mathbf{K}_{\text{T}}^{eIJ} &:= \int_{\mathcal{B}_0^e} \mathbf{B}_{\eta}^{IJ} + \mathbf{B}_{\kappa}^{IJ} \, dV\end{aligned}\quad (43)$$

contain the above discussed 10 terms.  $\mathbf{B}_{\delta}^{IJ}$  to  $\mathbf{B}_{\kappa}^{IJ}$  are given detailed in the appendix.

## 4 Magnetic loading with large deformation

Net couples  $\tilde{\mathbf{d}}$  are known from electro- and magnetostatics given by

$$\tilde{\mathbf{d}} = \vec{\mathbf{P}} \times \vec{\mathbf{E}} + \vec{\mathbf{M}} \times \vec{\mathbf{H}}, \quad (44)$$

see e.g. Eringen & Maugin [8]. Thus, a material with electric polarization  $\vec{\mathbf{P}}$  receives in general twisting moments within an electric field  $\vec{\mathbf{E}}$  and the torque of a compass needle is an example for the effect of materials with permanent magnetization  $\vec{\mathbf{M}}$  in an outer magnetic causing  $\vec{\mathbf{H}}$ . The twisting moment vanishes completely if the magnetization  $\vec{\mathbf{M}}$  of the compass needle is parallel to the outer magnetic field. The twisting moment becomes a maximum if magnetization and outer magnetic field are perpendicular. Orientation changes of the polarized or magnetized material can be coupled to net couples from Eq. (44) according to

$$\mathbf{d} = (\bar{\mathbf{R}} \vec{\mathbf{P}}) \times \vec{\mathbf{E}} + (\bar{\mathbf{R}} \vec{\mathbf{M}}) \times \vec{\mathbf{H}}. \quad (45)$$

In this paper we reduce Eq. (45) to  $\mathbf{d} = \bar{\mathbf{R}} \vec{\mathbf{M}} \times \vec{\mathbf{H}}$  for magnetic materials, since it is trivial to replace  $\vec{\mathbf{M}}$  through  $\vec{\mathbf{P}}$  resp.  $\vec{\mathbf{H}}$  through  $\vec{\mathbf{E}}$  for electrostatic problems. Further, we assume the irreversible magnetization  $\vec{\mathbf{M}}$  to be independent of  $\vec{\mathbf{H}}$  to leave the problem as simple as possible. In the practical examples of Section 5 this assumption can be fulfilled.

The virtual external work

$$\delta \Pi_{\mathbf{d}}^{ext} = - \int_{\mathcal{B}_0} \langle \mathbf{d}, \mathbf{w} \rangle dV \quad (46)$$

extends Eq. (22) and describes the variation of outer work done by net couples  $\mathbf{d}$ . With the reformulation of

$$\langle \mathbf{d}, \mathbf{w} \rangle = \langle \bar{\mathbf{R}} \vec{\mathbf{M}} \times \vec{\mathbf{H}}, \mathbf{w} \rangle = \bar{R}_{ab} \vec{M}_b \epsilon_{iac} \vec{H}_c \bar{w}_i = \vec{M}_b \vec{H}_c \bar{R}_{ba}^T W_{ac}^T = \underbrace{\langle \vec{\mathbf{M}} \otimes \vec{\mathbf{H}}, \bar{\mathbf{R}}^T \mathbf{W}^T \rangle}_{:=\mathbf{D}} \quad (47)$$

it is convenient to include the magnetostatic coupling through  $\mathbf{D} = \vec{\mathbf{M}} \otimes \vec{\mathbf{H}}$ , whereas  $\vec{\mathbf{M}}$  represents the given magnetization in the initial state on  $\mathcal{B}_0$ . The separation of  $\mathbf{w}$  goes by

$$\begin{aligned} \langle \mathbf{D}, \bar{\mathbf{R}}^T \mathbf{W}^T \rangle &= \langle \mathbf{D}^T, \mathbf{W} \bar{\mathbf{R}} \rangle = D_{ac}^T W_{ab} \bar{R}_{bc} = w_i \epsilon_{iab} \bar{R}_{bc} D_{ca} = \mathbf{w}^I \cdot \mathbf{B}_\varphi^I \\ &\text{with } \mathbf{B}_\varphi^I = \boldsymbol{\epsilon} : \bar{\mathbf{R}} \cdot \mathbf{D} N^I \quad . \end{aligned} \quad (48)$$

Thus, the element vector from Eq. (27b) extend to

$$\mathbf{R}_V^{eI} = \int_{\mathcal{B}_0^e} \mathbf{l}_0 N^I - \mathbf{B}_\beta^I + \mathbf{B}_\varphi^I dV + \int_{\partial \mathcal{B}_0^e} \mathbf{c}_0 N^I dA \quad . \quad (49)$$

The linear change of virtual external work in Eq. (46) at the point of evolution  $p^*$  reads

$$\Delta \delta \Pi_{\mathbf{d}}^{ext} = - \int_{\mathcal{B}_0} \Delta \langle \mathbf{d}, \mathbf{w} \rangle dV = - \int_{\mathcal{B}_0} \Delta \langle \mathbf{D}^T, \mathbf{W} \bar{\mathbf{R}} \rangle dV = \int_{\mathcal{B}_0} - \langle \mathbf{D}^T, \mathbf{W} \mathbf{Y} \bar{\mathbf{R}} \rangle dV \quad (50)$$

and gives an additional contribution to the stiffness matrix. Separation of  $\mathbf{w}$  and  $\mathbf{y}$  results in

$$\begin{aligned} - \langle \mathbf{D}^T, \mathbf{W} \mathbf{Y} \bar{\mathbf{R}} \rangle &= - D_{ab}^T W_{ac} Y_{cd} \bar{R}_{db} = - D_{ab}^T \epsilon_{rac} w_r \epsilon_{kcd} y_k \bar{R}_{db} = \mathbf{w}^I \cdot \mathbf{B}_\omega^{IJ} \cdot \mathbf{y}^J \\ &\text{with } \mathbf{B}_\omega^{IJ} = N^I \epsilon_{rca} D_{ba} \bar{R}_{db} \epsilon_{cdk} N^J \mathbf{e}_r \otimes \mathbf{e}_k \quad . \end{aligned} \quad (51)$$

Thus, the extension of the element stiffness matrix  $\mathbf{K}_T^{eIJ}$  in Eq. (43) yields

$$\mathbf{K}_T^{eIJ} := \int_{\mathcal{B}_0^e} \mathbf{B}_\eta^{IJ} + \mathbf{B}_\kappa^{IJ} + \mathbf{B}_\omega^{IJ} dV \quad . \quad (52)$$

Obviously, the efforts to extend this micropolar model for magnetic loading is low, even in the case of large deformation.

## 5 Numerical examples

### 5.1 Simple magnetic test

A cube under magnetic loading shows the capability of the model within a simple test. First, we consider the cube rigid and vary the direction of the homogeneous initial magnetization  $\vec{\mathbf{M}}$  concerning to the homogeneous and fixed outer magnetic causing  $\vec{\mathbf{H}}$ . The cube has unit length and an initial angle  $\alpha$  describes the direction of  $\vec{\mathbf{M}}$ , see Fig. 1 (left).

Because of the (assumed near) rigidity of the cube it holds  $\bar{\mathbf{R}} = \mathbb{1}$ , thus the outer moment is calculated altogether through

$$L = \left\| \int_{\mathcal{B}_0} \bar{\mathbf{R}} \vec{\mathbf{M}} \times \vec{\mathbf{H}} \, dV \right\| = \|\vec{\mathbf{M}}\| \|\vec{\mathbf{H}}\| \cos[\alpha]. \quad (53)$$

In Fig. 1 (middle) reaction forces  $A$  for  $-\pi/2 < \alpha < \pi/2$  are shown. For  $\pi/2 < \alpha < 3\pi/2$  they reverse their direction. Our finite element computation uses plain strain, an elastic modulus  $E = 10000$ , Poisson's ratio  $\nu = 0.3$  and 36 elements with linear shape functions. We observe for any  $\alpha$  the expected reaction forces with magnitude  $A = \|\vec{\mathbf{M}}\| \|\vec{\mathbf{H}}\| \cos[\alpha]/4$ . Next, we

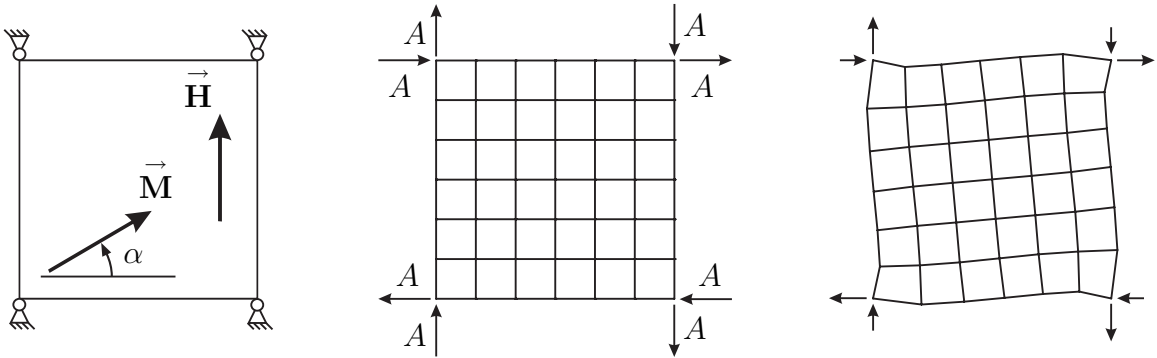


Figure 1: Left: Boundary conditions and loading. Middle: Reaction forces of the rigid body and  $-\pi/2 < \alpha < \pi/2$ . Right: Deformation and reaction forces for flexible material,  $\alpha = 45^\circ$ .

reduce the elastic modulus of the cube by factor 1000, thus it is no longer rigid. The plausible deformation is shown in Fig. 1 (right) for the initial angle  $\alpha = 45^\circ$ . The overall moment decrease to 88% of  $L$  from Eq. (53), caused by the body deformation.

### 5.2 Flexible magnetic stripe

This example investigates a flexible, magnetic stripe for its potential as actuator or switch. The stripe is made of NIB particles within an elastomer matrix.

Magnetic properties of the structure are gathered from the data sheet of a well-known manufacturer<sup>5</sup>. The material distinguishes itself with a high remanent magnetic field of  $B_r = 365 \text{ mT}$  and a high coercive magnetic strength of  $\vec{\mathbf{H}}_c = 580 \text{ kA/m}$ . Therefore, an external magnetic field of about 7 T (measured in the surrounding air) is necessary to demagnetize

<sup>5</sup>Max Baermann, Bergisch Gladbach

the stripe at room temperature. Exposing the stripe external magnetic fields beneath 1.6 T leads only to slight change in its magnetization. Own measurements yield an elastic modulus of  $E = 300\text{N/mm}^2$  and the Poissons ratio is estimated to  $\nu = 0.45$ .

In the undeformed state the stripe is  $d = 0.5\text{mm}$  thin and possesses an overall length of  $2L = 40\text{mm}$ . The width of the stripe is insignificant, further we consider plain strain for our computation. A longitudinal section of the undeformed stripe and its boundary conditions are shown in Fig. 2. The curved segment is characterized by the length of arch  $L$ , the dimension  $a = 0.35L$  and the magnetization  $\|\vec{\mathbf{M}}_1\| = B_r/10$  in negative  $x$ -direction. The straight segment with length  $L$  has magnetization  $\|\vec{\mathbf{M}}_2\| = B_r$  in negative  $y$ -direction. The structure is loaded by a homogeneous external magnetic causing  $\lambda \vec{\mathbf{H}}$ , producing in the surrounding air a magnetic field of  $\lambda \vec{\mathbf{B}} = \lambda \mu_0 \vec{\mathbf{H}} \cong \lambda 4\pi 10^{-7} \vec{\mathbf{H}}$ . We do not consider disturbances in the external magnetic field by the stripe.

Each segment of the structure is divided into 50 finite elements. Thus, 100 finite elements with quadratic shape functions are used in this model. It behaves nearly locking-free in performed bending tests. The deformation of the structure for increasing outer magnetic field  $\lambda \vec{\mathbf{B}}$  is

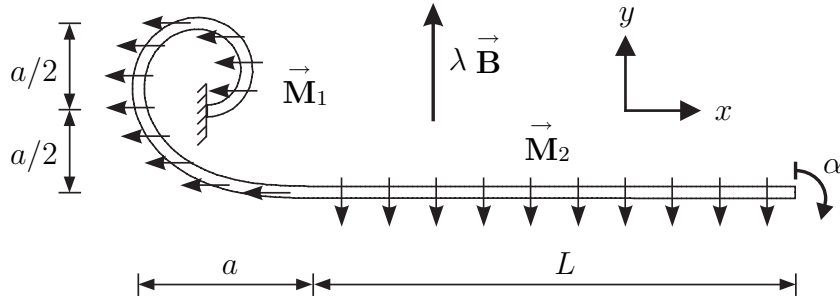


Figure 2: Longitudinal section and boundary conditions of the undeformed stripe.

shown in Fig. 3 (left). The magnetic field in the surrounding air reaches 1 Tesla for  $\lambda = 1$ .

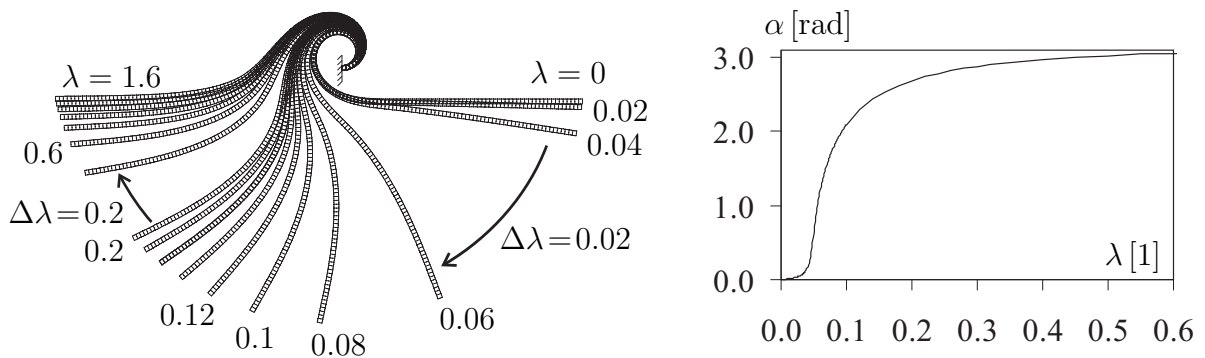


Figure 3: Left: Progress of deformation for increasing outer magnetic field  $\lambda \vec{\mathbf{B}}$ . Right: Rotation angle  $\alpha$  at the end of the stripe in dependence on loading factor  $\lambda$ .

First, the straight segment receives no loading since outer magnetic field and magnetization of the structure is parallel. However, the curved segment receives loading and rotates the straight segment by degrees. Therefore, the deformation increase more and more and leads to strong nonlinear behaviour, which is plotted in Fig. 3 (right) for the rotation angle  $\alpha$  at

the end of the stripe. When  $\alpha \rightarrow \pi$  the structure approaches a half round and therefore the loading disappears within the straight segment.

We conclude that the presented structure has high potential as electro-mechanical switch or valve. With small outer magnetic fields about  $\lambda \vec{\mathbf{B}} \approx 0.1 \text{ T}$  large deformations can be reached. Further, the loading through an outer magnetic field and the resistance of the stripe against acid loading may be an important advantage.

### 5.3 Snap through of a cone shell

A cone shell made of the same material like in Subsection 5.2 is investigated on its function as valve. Therefore, the shell presses its seal onto an o-ring, see Fig. 5.

Shell and seal are remanent magnetized with  $\|\vec{\mathbf{M}}\| = B_r = 365.4 \text{ mT}$  in negative  $z$ -direction, as shown in Fig. 4 resp. Fig. 5.

With respect to symmetry only a quarter of the system is modeled by  $4 \times 6$  finite elements in plane and with one element through the thickness. Quadratic shape functions are used, note that visualization lay a mesh through all nodes. In  $xz$ -plane the displacements in  $y$ -direction and the rotations around  $x$ - and  $z$ -axis are set to zero. Further, in  $yz$ -plane the displacements in  $x$ -direction and the rotations around  $y$ - and  $z$ -axis are set to zero.

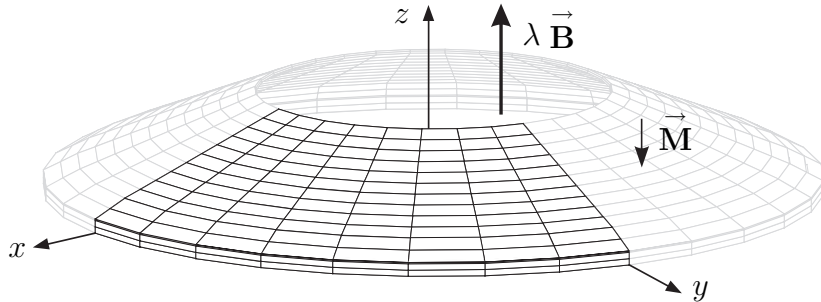


Figure 4: Magnetic cone shell with magnetisation  $\vec{\mathbf{M}}$  and loading  $\lambda \vec{\mathbf{B}}$ .

A homogeneous external magnetic causing  $\lambda \vec{\mathbf{H}}$ , which produces in air a magnetic field with magnitude  $\lambda \vec{\mathbf{B}} \cong 4 \pi 10^{-7} \lambda \vec{\mathbf{H}}$  acts on cone and seal. For  $\lambda = 1$  the flux density reaches the absolute value of one Tesla. This field can be produced by a copper wire coil outside the valve. Thus, neither mechanical components nor electrical components are necessary within the valve.

Dimensions of the valve can be seen as sectional drawing S1 in Fig. 5. The thickness of the shell amount  $t = 0.1 \text{ mm}$ , the other sizes are  $r_1 = 5 \text{ mm}$ ,  $r_2 = 10 \text{ mm}$ ,  $r_3 = 10.2 \text{ mm}$ ,  $r_4 = 11 \text{ mm}$ ,  $h_1 = 0.4 \text{ mm}$ ,  $h_2 = 0.8 \text{ mm}$  and  $h_3 = 2.4 \text{ mm}$ .

The sectional drawing S1 shows the o-ring (grey) in initial contracted condition. A fictitious force  $F_f = 2.1 \text{ N}$  compresses the o-ring into this initial position. So, the contact force  $F_k$  between seal and o-ring is zero and the cone is undeformed. By removing  $F_f$  a natural state of equilibrium appears, as can be seen in the sectional drawing S2 of Fig. 5. In this state, the contact force between seal and o-ring reaches  $F_k \cong 1 \text{ N}$ . Caused by the valve's deformation the direction of the permanent magnetic field  $\vec{\mathbf{M}}$  changes.

As soon as the seal lift-off from the o-ring, the o-ring is stress free and we measure the height  $2.3 h_1$ . That means, the o-ring is compressed in the initial state by the strain  $\varepsilon =$

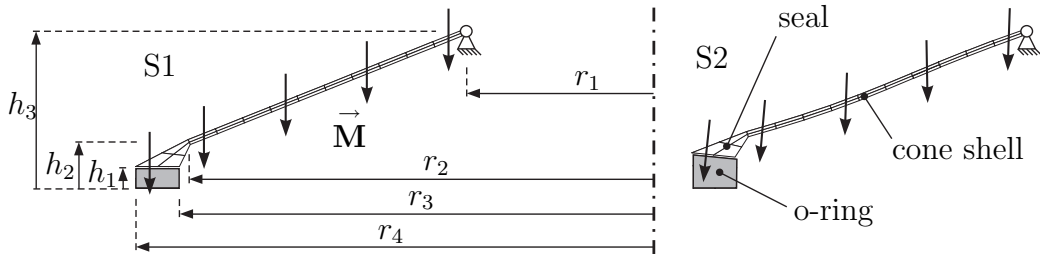


Figure 5: Sectional drawings of the valve in initial state (S1) and for  $\lambda = 0$  (S2).

$(h_1 - 2.3 h_1)/(2.3 h_1) = -0.57$ . For the sake of simplicity, we do not take frictional forces between seal and o-ring into account.

We use the vertical displacement  $u$  at the bottom of the seal for the load-displacement diagram in Fig. 6. It is the result of a computation with an arc-length method. Prominent points in the diagram are marked with S1 to S8. In Fig. 5 resp. Fig. 7 every prominent point is shown with its sectional drawing.

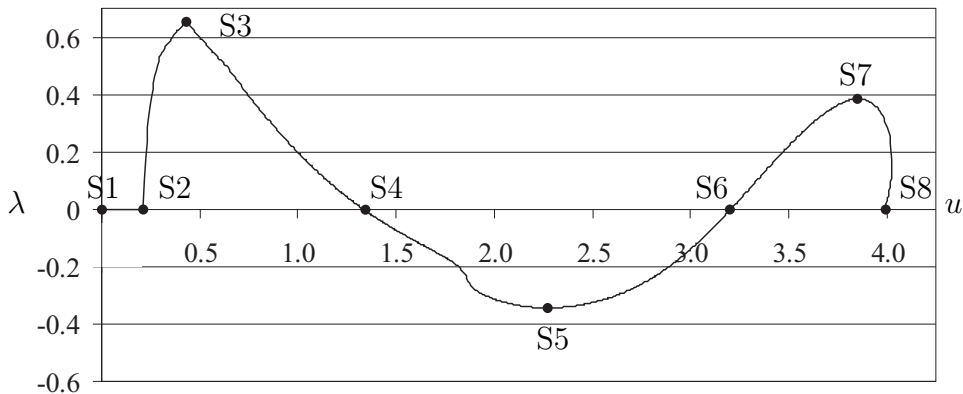


Figure 6: Load-displacement diagram for vertical displacement  $u$  from a computation with arc-length method. Prominent points are marked with sectional drawing numbers S1 to S8.

The load-displacement diagram in Fig. 6 shows that standard magnetic flux densities  $\lambda \vec{\mathbf{B}}$  are sufficient to open and close the valve. The cone snaps-through and remains in open or closed position without outer magnetic fields. With the load factor  $\lambda = 0.66$  resp.  $\lambda = -0.34$  the valve can be opened or closed. The distance between seal and o-ring is at least 3 mm.

## 6 Summary

In this work a geometrically exact and materially non-linear micropolar model including magnetic loading has been presented. We use explicit rotations to take large deformation and its consequences to the loading into account. Since the magnetization direction of the structure depends on deformation also the loading does. This can be used to design structures for switches and valves. They can be advantageous especially for small components or within corrosive environment. Here, Neodymium Iron Boron particles bonded within an elastomer matrix are promising for practical applications.

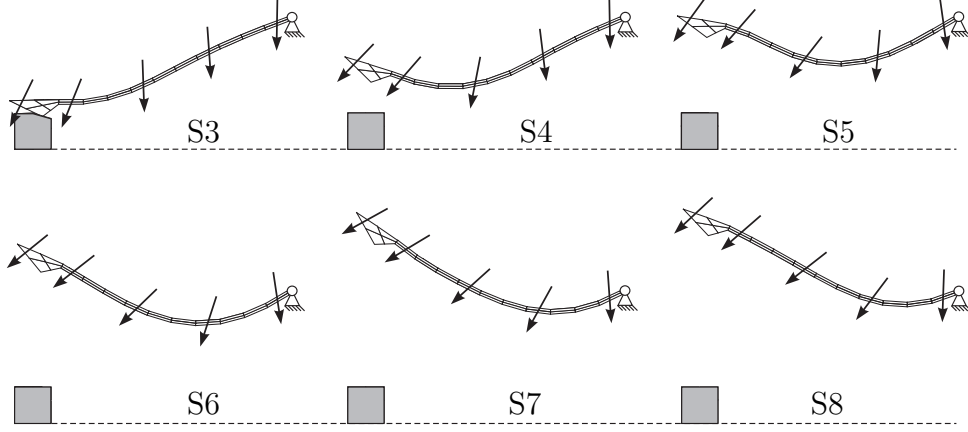


Figure 7: Sectional drawings S3 to S8 corresponding to Fig. 6.

In the continuum theory of our model, it is a crucial point to treat the angular momentum equation explicitly and allow for non-symmetric Cauchy stresses. Our suggestion for the material parameters is as simple as possible and reduces to the classical Lamé parameters and one additional micropolar parameter. Then, the model allows for classical elasticity, which is not sensitive concerning this micropolar parameter  $\mu_c$ . It is obvious to choose  $\mu_c = \mu$ , but  $\mu_c > \mu$  is also tested without worth mentioning influence.

The right hand side and tangent stiffness matrix for the Newton-Raphson algorithm within the finite element formulation is given in detail. In general 6 degrees of freedom appear at every node. These are the components of the displacement field and the components of the rotation field. They are geometrically coupled through the strain measure in Eq. (7). Anyway, the special parameter choice of  $\mu_c = \mu$  acts like a direct spring between the rotation field and the orthogonal part from the polar decomposition of the deformation gradient  $\mathbf{F}$ , since skew-symmetrical parts of strain are suppressed as far as possible. Therefore, it is misleading to speak about an independent rotation field. Strictly speaking, the angular momentum equation asks for rotational parameters and enhances the theory by allowing net couples. The coupling between rotations and stresses is of minor matter.<sup>6</sup>

The effort to program the right hand side and tangent stiffness matrix for a finite element program is shown in this paper. Further, it is expensive to compute 6 degrees of freedom at each node. But the introduction of this sort of magnetic loading is obviously natural and without complications.

## Appendix

Details for the element stiffness matrices in Eq. (43) are given below.

$$\text{Term 1: } (\bar{\mathbf{R}}^T \delta \mathbf{F}) : \mathbf{C} : (\bar{\mathbf{R}}^T \Delta \mathbf{F}) = \bar{R}_{ar}^T \delta u_{r,b} \mathbf{C}_{abcd} \bar{R}_{ck}^T \Delta u_{k,d} = \delta \mathbf{u}^I \cdot \mathbf{B}_\delta^{IJ} \cdot \Delta \mathbf{u}^J$$

$$\text{with } \mathbf{B}_\delta^{IJ} := \bar{R}_{ra}^I N_b^I \mathbf{C}_{abcd} \bar{R}_{kc}^J N_d^J \mathbf{e}_r \otimes \mathbf{e}_k.$$

$$\text{Term 2: } (\bar{\mathbf{R}}^T \delta \mathbf{F}) : \mathbf{C} : (\bar{\mathbf{R}}^T \mathbf{Y}^T \mathbf{F}) = \bar{R}_{ar}^T \delta u_{r,b} \mathbf{C}_{abcd} \bar{R}_{cf}^T y_k \epsilon_{kfe} \mathbf{F}_{ed} = \delta \mathbf{u}^I \cdot \mathbf{B}_\epsilon^{IJ} \cdot \mathbf{y}^J$$

<sup>6</sup>Indeed, for  $\mu_c \rightarrow 0$  an additional kinematic appears within this continuum theory. Then, gradients of  $\bar{\mathbf{R}}$  need to be controlled and the model is put into an other context, e.g. plasticity theory.

with  $\mathbf{B}_\epsilon^{IJ} := N_b^I \bar{R}_{ra} \mathbf{C}_{abcd} \bar{R}_{fc} \epsilon_{kfe} F_{ed} N^J \mathbf{e}_r \otimes \mathbf{e}_k$ .

Term 3:  $(\bar{\mathbf{R}}^T \mathbf{W}^T \mathbf{F}) : \mathbb{C} : (\bar{\mathbf{R}}^T \Delta \mathbf{F}) = \mathbf{w}^I \cdot (\mathbf{B}_\epsilon^{JI})^T \cdot \Delta \mathbf{u}^J$  with

$(\mathbf{B}_\epsilon^{JI})^T = N_{,b}^J \bar{R}_{ra} \mathbf{C}_{abcd} \bar{R}_{fc} \epsilon_{kfe} F_{ed} N^I \mathbf{e}_k \otimes \mathbf{e}_r = N_{,b}^J \bar{R}_{ka} \mathbf{C}_{abcd} \bar{R}_{fc} \epsilon_{rfe} F_{ed} N^I \mathbf{e}_r \otimes \mathbf{e}_k$ .

Term 4:  $(\bar{\mathbf{R}}^T \mathbf{W}^T \mathbf{F}) : \mathbb{C} : (\bar{\mathbf{R}}^T \mathbf{Y}^T \mathbf{F}) = \bar{R}_{ae}^T w_r \epsilon_{ref} F_{fb} \mathbf{C}_{abcd} \bar{R}_{cg}^T y_k \epsilon_{kgh} F_{hd} = \mathbf{w}^I \cdot \mathbf{B}_\eta^{IJ} \cdot \mathbf{y}^J$

with  $\mathbf{B}_\eta^{IJ} := N^I \bar{R}_{ea} \epsilon_{ref} F_{fb} \mathbf{C}_{abcd} \bar{R}_{gc} \epsilon_{kgh} F_{hd} N^J \mathbf{e}_r \otimes \mathbf{e}_k$ .

Term 5:  $\langle \mathbf{S}_1^{\text{lin}}, \mathbf{Y} \mathbf{W} \mathbf{F} \rangle = S_{1ab}^{\text{lin}} y_k \epsilon_{kac} w_r \epsilon_{rcd} F_{db} = \mathbf{w}^I \cdot \mathbf{B}_\kappa^{IJ} \cdot \mathbf{y}^J$

with  $\mathbf{B}_\kappa^{IJ} := N^I \epsilon_{rcd} S_{1ab}^{\text{lin}} F_{db} \epsilon_{kac} N^J \mathbf{e}_r \otimes \mathbf{e}_k$ .

Term 6:  $\langle \mathbf{S}_1^{\text{lin}}, \mathbf{W}^T \Delta \mathbf{F} \rangle = S_{1ab}^{\text{lin}} w_r \epsilon_{rak} \Delta u_{k,b} = \mathbf{w}^I \cdot \mathbf{B}_\lambda^{IJ} \cdot \Delta \mathbf{u}^J$

with  $\mathbf{B}_\lambda^{IJ} := N^I S_{1ab}^{\text{lin}} \epsilon_{rak} N_{,b}^J \mathbf{e}_r \otimes \mathbf{e}_k$ .

Term 7:  $\langle \mathbf{S}_1, \mathbf{Y}^T \delta \mathbf{F} \rangle = S_{1ab} y_k \epsilon_{kar} \delta u_{r,b} = \delta \mathbf{u}^I \cdot \mathbf{B}_\omega^{IJ} \cdot \mathbf{y}^J$

with  $\mathbf{B}_\omega^{IJ} := N_b^I S_{1ab} \epsilon_{kar} N^J \mathbf{e}_r \otimes \mathbf{e}_k$ .

Term 8:  $\hat{\mathbf{C}}_{\text{det}} \langle \delta \mathbf{F}, \mathbf{F}^{-T} \rangle \langle \mathbf{F}^{-T}, \Delta \mathbf{F} \rangle = \hat{\mathbf{C}}_{\text{det}} \delta u_{r,a} F_{ra}^{-T} F_{kb}^{-T} \Delta u_{k,b} = \delta \mathbf{u}^I \cdot \mathbf{B}_\theta^{IJ} \cdot \Delta \mathbf{u}^J$

with  $\mathbf{B}_\theta^{IJ} := \hat{\mathbf{C}}_{\text{det}} N_{,a}^I F_{ar}^{-1} F_{bk}^{-1} N_{,b}^J \mathbf{e}_r \otimes \mathbf{e}_k$ .

Term 9:  $-\mathbf{C}_{\text{det}} \langle \delta \mathbf{F}, \mathbf{Y} \mathbf{F}^{-T} \rangle = -\mathbf{C}_{\text{det}} \delta u_{r,a} (-y_k) \epsilon_{krb} F_{ba}^{-T} = \delta \mathbf{u}^I \cdot \mathbf{B}_\vartheta^{IJ} \cdot \Delta \mathbf{u}^J$

with  $\mathbf{B}_\vartheta^{IJ} := -\mathbf{C}_{\text{det}} N_{,a}^I F_{br}^{-1} F_{ak}^{-1} N_{,b}^J \mathbf{e}_r \otimes \mathbf{e}_k$ .

Term 10:  $-\mathbf{C}_{\text{det}} \langle \delta \mathbf{F}, \mathbf{F}^{-T} \Delta \mathbf{F}^T \mathbf{F}^{-T} \rangle = -\mathbf{C}_{\text{det}} \delta u_{r,a} F_{rb}^{-T} \Delta u_{k,b} F_{ka}^{-T} = \delta \mathbf{u}^I \cdot \mathbf{B}_\iota^{IJ} \cdot \mathbf{y}^J$

with  $\mathbf{B}_\iota^{IJ} := -\mathbf{C}_{\text{det}} N_{,a}^I \epsilon_{kbr} F_{ab}^{-1} \mathbf{e}_r \otimes \mathbf{e}_k$ .

## References

- [1] W.B. Anderson and R.S. Lakes. *Size effects due to Cosserat elasticity and surface damage in closed-cell polymethacrylimide foam*. J. Mat. Sci., **29**: 6413–6419, 1994.
- [2] N. Büchter and E. Ramm. *Shell theory versus degeneration - a comparison in large rotation finite element analysis*. Int. J. Num. Meth. Engng., **34**: 39–59, 1992.
- [3] H. Buefler. *On drilling degrees of freedom in nonlinear elasticity and a hyperelastic material description in terms of the stretch tensor*. Part I: Theory. Acta Mech., **113**: 21–35, 1995.
- [4] S. Cleja-Tigoio. *Couple stresses and non-Riemannian plastic connection in finite elastoplasticity*. Z. Angew. Math. Phys., **53**: 996–1013, 2002.
- [5] E. Cosserat and F. Cosserat. *Théorie des corps déformables*. Librairie Scientifique A. Hermann et Fils, Paris, 1909. English translation from D. Delphenich, 2007.
- [6] S. Diebels, H. Steeb and W. Ehlers. *Microscopic and macroscopic modelling of foams*. Proc. Appl. Math. Mech., **2**: 156–157, 2003.
- [7] J. Dyszlewicz. *Micropolar Theory of Elasticity*. Lecture Notes in Applied and Computational Mechanics, volume 15, Springer, Heidelberg, 2004.

- [8] A.C. Eringen and G.A. Maugin. *Electrodynamics of Continua I - Foundations and Solid Media*. Springer, Heidelberg, 1989.
- [9] A. C. Eringen. *Microcontinuum Field Theories*. Springer, Heidelberg, 1999.
- [10] N.A. Fleck, G.M. Müller, M.F. Ashby and J.W. Hutchinson. *Strain gradient plasticity: theory and experiment*. Acta. Metall. Mater., **42(2)**: 475–487, 1994.
- [11] J.C. Simo, D.D. Fox and T.J.R. Hughes. *Formulations of finite elasticity with independent rotations*. Comp. Meth. Appl. Mech. Engrg., **95**: 277–288, 1992.
- [12] P. Grammenoudis and C. Tsakmakis. *Predictions of microtorsional experiments by micropolar plasticity*. Proc. Roy. Soc. London A, **461**: 189–205, 2005.
- [13] K.H. Hofmann and S.A. Morris. *The structure of compact groups*. Studies in Mathematics, deGruyter, Berlin, 1998.
- [14] G.A. Maugin. *On the structure of the theory of polar elasticity*. Phil. Trans. Roy. Soc. London A, **356**: 1367–1395, 1998.
- [15] T. Merlini. *A variational formulation for finite elasticity with independent rotation and Biot-axial field*. Comp. Mech., **19**: 153–168, 1997.
- [16] I. Münch. *Ein geometrisch und materiell nichtlineares Cosserat-Modell - Theorie, Numerik und Anwendungsmöglichkeiten*. Institut für Baustatik, Dissertation, Universität Karlsruhe, Download: <http://digbib.ubka.uni-karlsruhe.de/volltexte/1000007371>, 2007.
- [17] P. Neff. *Existence of Minimizers for a finite-strain micromorphic elastic solid*. Proc. Roy. Soc. Edinb. **136A**: 997–1012, 2006.
- [18] P. Neff and S. Forest. *A geometrically exact micromorphic model for elastic metallic foams accounting for affine microstructure. Modelling, existence of minimizers, identification of moduli and computational results*. J. Elasticity, **136**: 997-1012, 2006.
- [19] P. Neff and I. Münch. *Curl bounds Grad on SO(3)*. ESAIM: Control, Optimisation and Calculus of Variations, published online, DOI: 10.1051/cocv:2007050, **14(1)**: 148–159, 2007.
- [20] P. Neff. *A finite strain elasto-plastic Cosserat theory for polycrystals with grain rotations*. Int. J. Engng. Sci. **87**: 239-276, 2007.
- [21] P. Neff, A. Fischle and I. Münch. *Symmetric Cauchy-stresses do not imply symmetric Biot-strains in weak formulations of isotropic hyperelasticity with rotational degrees of freedom*. Acta Mechanica, published online DOI 10.1007/s00707-007-0509-x, 2007.
- [22] W. Pietraszkiewicz and J. Badur. *Finite rotations in the description of continuum deformation*. Int. J. Engng. Science, **9**: 1097–1115, 1983.
- [23] C. Sansour and W. Wagner. *Multiplicative updating of the rotation tensor in the finite element analysis of rods and shells, a path independent approach*. Comp. Mech., **31**: 153–162, 2003.

- [24] J. Schröder and P. Neff. *Invariant formulation of hyperelastic transverse isotropy based on polyconvex free energy functions*. *Int. J. Solids Struct.* **40(2)**: 401–445, 2003.
- [25] W. Wagner and F. Gruttmann. *A robust nonlinear mixed hybrid quadrilateral shell element*. *Int. J. Num. Meth. Engng.* **64**: 635-666, 2005.
- [26] K. Wisniewski. *A shell theory with independent rotations for relaxed Biot stress and right strain*. *Comp. Mech.*, **21(2)**: 101–122, 1998.